Available online at www.sciencedirect.com
SCIENCE DIRECT
Catalysis Today 106 (2005) 227–232
CATALYSIS TODAY
www.elsevier.com/locate/cattod

Scaling down trickle bed reactors

Daniël van Herk, Michiel T. Kreutzer, Michiel Makkee *, Jacob A. Moulijn

Reactor & Catalysis Engineering, Delft University of Technology, Julianalaan 136, NL 2628 BL Delft, The Netherlands

Abstract

The scaling down of trickle bed reactors for catalyst testing in deep hydrodesulphurisation (HDS) is evaluated. A multiphase micro-reactor system has been built specifically for HDS, consisting of a set of six 2 mm diameter packed beds with particles of approximately 100 μm. To confirm plug-flow behaviour (for integral conversion) and to guarantee the measurement of true kinetics, the hydrodynamics have to be investigated.

For this purpose, a 'cold-flow' set-up of the same dimensions as the HDS reactors, has been built. A liquid feed with a dye tracer pulse as well as gas are fed to a glass column, packed with glass particles. From the recorded outlet concentration, the influence of the gas- and liquid-flow rate on the mean residence time and residence-time distribution (RTD) have been determined.

This hydrodynamics investigation describes the deviation from plug flow in micro-scale packed beds. The results show that the deviations from plug flow are minimal. The effect of the gas-flow rate on the liquid-residence time is more pronounced in micro-packed beds than that in trickle beds with larger particles.

The RTD study presented here provides valuable insight into the behaviour of scaled-down kinetic-test facilities.

Keywords: Trickle bed; Scaling down; RTD; Axial dispersion; Micro-packed bed; Hydrodynamics; HDS

1. Background

As the fuel legislation becomes increasingly stringent, the oil industry needs to desulphurise to ever decreasing sulphur levels. Measuring catalyst performance and kinetics of complex mixtures over the entire range of conversion, from differential to integral, eliminates extrapolation and improves reliability of performance measurements. Furthermore, the ongoing improvements of hydrodesulphurisation (HDS) catalysts have progressed to a level that, under industrial conditions, concentration gradients due to intra-particle diffusion become relevant. As a result, the shaped particles used in commercial trickle beds are less suited for kinetic studies. The context of this work is the need for kinetic-test facilities for deep HDS catalysts in powder form.

For measuring intrinsic kinetics, temperature and concentration gradients on the scale of the particle have to be absent. The bed needs to be isothermal and the reactor should behave as a plug-flow reactor. The latter is in particular important for deep desulphiding where extremely high conversion is aimed at. These requirements imply using small particles and a sufficient bed length. For flow through such small particles, surface tension forces become much more important and established trickle-bed correlations cannot be extrapolated. For a reliable design of the reactor bed and for a choice of window of operation the hydrodynamics of such packed-bed micro-reactors have to be investigated.

The multiphase micro-reactor system that has been built specifically for this work consists of six parallel reactors with an inner diameter of 2 mm, packed with particles of approximately 100 μm. The feed contains a representative liquid feed and a H_2/H_2S mixture as gas feed. A gas chromatograph performs the analysis of the liquid phase. The system can operate as a differential or an integral reactor. It is a design, based on the gas-only catalyst six-flow units described in literature, e.g. [1], improved and modified for the kinetic testing of multiphase processes.

For a study of the kinetics, it is very important to have a well-defined catalyst and a well-defined ideal reactor. When

* Corresponding author. Tel.: +31 15 278 1391; fax: +31 15 278 5006.
E-mail address: m.makkee@tnw.tudelft.nl (M. Makkee).

0920-5861/$ – see front matter
doi:10.1016/j.cattod.2005.07.180

Nomenclature

A	absorbance (a.u.)
b	path length (m)
C	concentration (gm *tracer*/gm *ethanol*)
D_{ax}	axial-dispersion coefficient (m^2/s)
d_p	particle diameter (m)
I	light intensity (a.u.)
L	column length (m)
n	reaction order [−]
N	equivalent number of mixers in series [−]
Pe_L	column Péclet number [−] Eq. (5)
Pe_p	particle Péclet number [−] Eq. (6)
Re_L	liquid Reynolds number [−]
Sc	Schmidt number [−]
u	superficial velocity (m/s)
X	conversion [−]

Greek

α	absorption coefficient [−]
σ_L^2	variance (s^2)
τ_L	mean residence time (s)
τ_θ	dimensionless mean residence time [−] Eq. (4)

Suffix

blank	without column
dark	no light source
g	gas
L	liquid
ref	reference (0% tracer)
tot	total (system + column)

realistic conditions are aimed at, it is good to realise that hydrocarbons, including the sulphur-containing hydrocarbons, can have fractions of up to 75% in the gas phase at typical HDS temperature and pressure. This has important implications for the design of catalyst testing units. For that, we need to understand: (i) the liquid-phase residence-time distribution (RTD), (ii) the gas-phase RTD, (iii) the rate of mass exchange between gas and liquid and (iv) the impact of wetting on kinetics. The first three aspects can be separately explored in cold-flow units. A priori, it is clear that plug-flow behaviour is preferred in which gas does not bypass the liquid.

2. RTD set-up

The 'cold-flow' set-up that has been built has the same dimensions as the reactors in the six-flow reactor system, but it is constructed out of glass for ease of visual observation. The cold-flow unit is operated at ambient conditions to investigate the axial dispersion, by measuring the RTD curves. It consists of a column, packed with glass spherical particles of 100 μm and a (HPLC) six-way valve for the liquid feed, capable of injecting 10 μL of coloured dye tracer pulse (Fig. 1). Ethanol has been used as the liquid phase, fed with an ISCO syringe pump in the range 50–500 μL/min (∼0.5–5.3 mm/s superficial velocity in the column). Nitrogen gas is fed to the column with two different mass-flow controllers covering the range of 1.6–84.9 mm/s (∼0.15–8.0 mL/min).

The effluent of the column is collected and its light intensity is determined with a spectrometer probe. Noise reduction has been a major concern. The fluctuations, found in the signal due to variations in the integration time, are solved by using the signal at 800 nm, unaffected by the tracer concentration, as an internal standard. The dye tracer, a highly concentrated solution of Coomassie Brilliant Blue G in ethanol, has a maximum absorbance at 600 nm. By dividing the values of the light intensity at these two wavelengths, a correction is made for the fluctuations. The relation between the light intensity (in arbitrary units) and the absorption is found with the Lambert–Beer law [2]:

$$A = \alpha \cdot b \cdot C = -\log\left(\frac{I - I_{dark}}{I_{ref} - I_{dark}}\right) \quad (1)$$

where A is the absorbance, α the wavelength-dependent absorption coefficient, b the path length, C the concentration, I the light intensity at concentration C, I_{dark} the light intensity with the light source turned off and I_{ref} is the light intensity with 0% tracer in the liquid.

With a calibration, the linear part of the relation between the absorption and the concentration is found. This absorption coefficient, together with a correction for the increase of the liquid volume in the collecting beaker downstream of the column during the run, allows the determination of the breakthrough curve of the tracer (the 'F-curve') in weight percentage. The mean residence time and the residence-time distribution are evaluated from the F-curve. The E-curve, which may be obtained by differentiating the F-curve, is less suitable since it is contaminated by a significant amount of noise, introduced by differentiating the

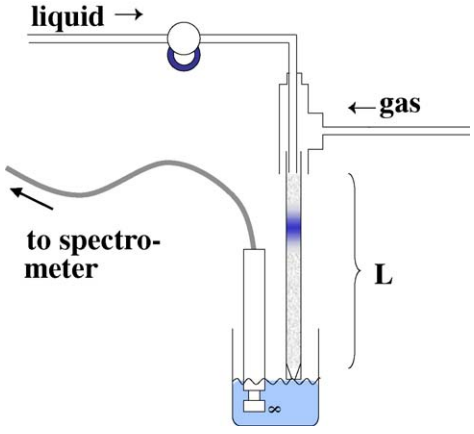

Fig. 1. Schematic view of the cold-flow set-up.

small error in the F-curve. Therefore, the measured data is analysed directly in the time domain without first converting to an E-curve. The first and second moment of the residence-time distribution are obtained from the F-curve using textbook methods [3]. The spread ($2\sigma_L$) is found from the difference between the time values at which 14 and 86% of the tracer has come out of the column. The mean residence time is evaluated by integrating $1 - F$ in the time domain.

3. Data analysis

To eliminate inlet and outlet effects, experiments are performed with and without a column installed. In this way, a correction is made for the tracer spread due to the injection system according to the following formulae [3]:

$$\sigma_L^2 = \sigma_{L,tot}^2 - \sigma_{L,blank}^2 \tag{2}$$

$$\tau_L = \tau_{L,tot} - \tau_{L,blank} \tag{3}$$

For correlation purposes, a dimensionless expression for the residence time (τ_θ) is formulated by dividing the measured residence time (τ_L) by a calculated value, based on the column length (L) and the total superficial velocity of both liquid and gas (u_{tot}). For the calculation of the superficial velocity, the void volume is needed. This volume has been determined independently for the packed column used in the experiments by measuring the difference in weight of a liquid filled packed column and a gas filled packed column:

$$\tau_\theta = \frac{\tau_L}{L/(u_g + u_L)} \tag{4}$$

With the variance (σ_L^2) and the residence time (τ_L) known, a dimensionless expression for the column dispersion number can be found. The reciprocal is often referred to as the column Péclet number (Pe_L):

$$Pe_L = \frac{2 \cdot \tau_L^2}{\sigma_L^2} = \frac{L \cdot u_L}{D_{ax}} \tag{5}$$

with D_{ax} as the axial-dispersion coefficient. When the particle diameter is used as characteristic length instead of the column length, this becomes:

$$Pe_p = \frac{d_p \cdot u_L}{D_{ax}} = Pe_L \cdot \frac{d_p}{L} \tag{6}$$

with Pe_p as the particle Péclet number and d_p as the particle diameter. Mears [4] proposed a criterion based on a deviation of the conversion of no more than 5% from the conversion under perfect plug-flow conditions for an adequately performing fixed-bed reactor (Eq. (7)). From this criterion, the minimal reactor length can be calculated at a given conversion, if the particle Péclet number is known.

$$Pe_L > 20 \cdot n \cdot \ln(1 - X)^{-1} \tag{7}$$

$$L > 20 \cdot n \cdot \ln(1 - X)^{-1} \frac{d_p}{Pe_p} \tag{8}$$

with n as the reaction order. Later, Gierman [5] suggested 10% as a more suitable cut-off criterion, and replaced the factor 20 in Eqs. (7) and (8) by a factor 8.

At high velocities in large-diameter trickle beds, i.e. at high Reynolds number (Re_L), the flow in a cavity between particles has sufficient secondary flow features, such as vortices and swirls, that the cavity may be described as an ideal stirrer. N particles in line behave as N stirrers-in-series and the particle Péclet number becomes 2. In micro-packed beds, with very low Reynolds numbers, inertia-induced secondary features will mostly be absent and secondary flow features have to be induced by the passing bubbles. The amounts of reported literature data for axial dispersion in multi-phase flow at low Re_L are very limited. In general, $Pe_p \ll 2$ is found, which indicates that the bubbles at low Re_L are not very effective at inducing mixing in the voids between particles.

4. Results

The RTD experiments performed with the set-up are reproducible. Representative breakthrough curves, measured at varying liquid and gas-flow rate, are shown in Fig. 2. The location and the slope of the middle part of the breakthrough curves are indicative of the residence time and residence-time distribution, respectively.

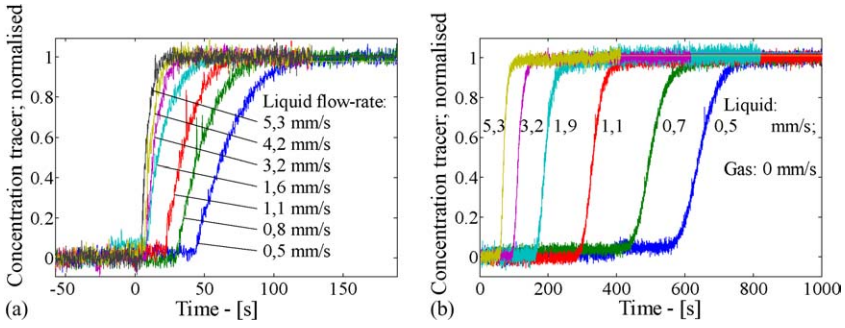

Fig. 2. Representative breakthrough curves of: (a) the system without column and (b) liquid-only experiments.

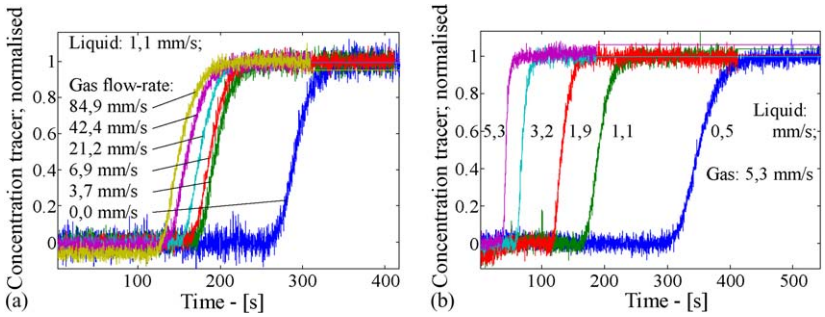

Fig. 3. Representative breakthrough curves of the liquid phase in gas/liquid experiments with: (a) varying gas-flow rates at a fixed liquid-flow rate and (b) varying liquid-flow rates at a fixed gas-flow rate.

Fig. 2(a) shows the breakthrough curves of the RTD measurements of the system without column at different liquid-flow rates. The data from these experiments are used to correct the results in Figs. 2(b) and 3(a and b) in order to provide information about the column only (Eqs. (2) and (3)).

At high flow rates, the difference between the inlet variance (calculated from the data in Fig. 2(a)) and total system variance is small and, as a consequence, unreliable data are produced. These values are disregarded in subsequent data-analysis.

In Fig. 2(b), showing the breakthrough curves from liquid-only experiments, it can be seen that the mean residence time decreases at increasing liquid-flow rate.

Fig. 3(a) shows a set of representative breakthrough curves at different gas-flow rates in which the liquid-flow rate is the same. Compared to the single-phase measurements the mean residence time is lower due to the presence of the gas phase, but the influence of different gas-flow rates is minimal. The slopes, or residence-time distributions are approximately unaffected. Fig. 3(b) shows the effect of varying liquid-flow rate at a constant gas-flow rate of 4.9 mm/s, comparable to Fig. 2(b), now in the presence of a gas flow.

In Fig. 4, the results of the data analysis are shown for liquid-only experiments. Fig. 4(a) shows the dimensionless residence time of Eq. (4) versus the liquid-flow rate and Fig. 4(b) shows the particle Péclet number (of Eq. (6)) versus the liquid Reynolds number. These results show the constant value of the Péclet number. The results on the residence time in gas–liquid experiments are plotted in Fig. 5. In this figure, the dimensionless residence time of the liquid (Eq. (4)) is plotted against the liquid fraction of the flow providing a correlation for all the combinations of flow rates. It shows that a decrease in the liquid fraction of the flow causes an exponential increase in the dimensionless residence time. At higher liquid fractions, this correlation approaches the value $\tau_\theta \sim 1$. In Fig. 5(b) a closer look is given. Fig. 6(a) shows the dimensionless axial dispersion in the form of the column Péclet number (defined in Eq. (5)) versus the gas-flow rate at different liquid-flow rates. In Fig. 6(b), these data are shown as the particle Péclet number versus the liquid fraction of the flow.

5. Discussion

5.1. Single-phase measurements

In the single-phase experiments, the liquid is expected to completely fill the column interstices. Therefore, the dimensionless residence time in single-phase experiments, as shown in Fig. 4(a), is expected to be 1. For the higher flow rates excellent agreement is found and the experimental residence time is accurate within two percent. At low liquid-flow rate, the experimental residence time is systematically lower than the expected value. The error is still within 5%. This deviation is probably due to a small volume of gas that remains in the column in the form of small bubbles in the interstitial space between particles. Apparently, at low flow rate, the liquid does not push all of these bubbles out. This small stagnant gas volume should be subtracted from the void volume that is available for the liquid to flow through. It will lead to the lower residence time.

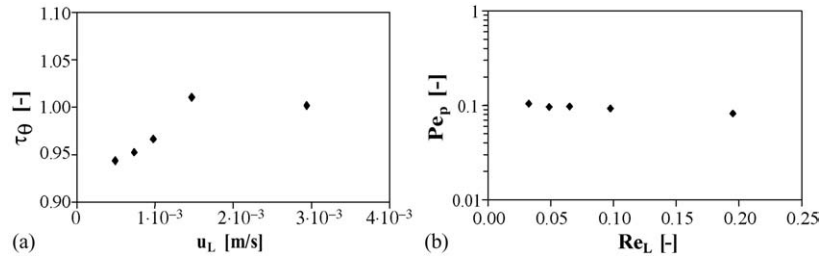

Fig. 4. The single-phase results (liquid-only) with: (a) the dimensionless residence time (τ_θ) vs. the liquid-flow rate and (b) the particle Péclet number (Pe_p) on a log scale vs. the Reynolds number.

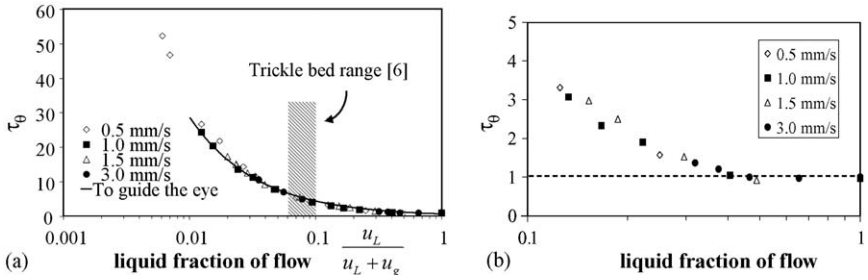

Fig. 5. Gas–liquid experiments with: (a) a correlation for the residence time. The liquid-flow rates are individually indicated by different symbols; (b) a closer look at high liquid-fraction area.

The Péclet numbers, obtained for single-phase experiments without gas flow, compare well with data reported [7,8]. The tracer used is a large molecule and the Schmidt number (Sc) is estimated to be $\sim 10^4$. Around $Re \sim 0.1$ or $ReSc \sim 1000$, the particle Péclet number remains constant for several decades of Re at $Pe_p \sim 0.1$ for the large Schmidt numbers in this work.

5.2. Two phase measurements—residence times

The residence times, as determined by the gas–liquid RTD measurements, provide information on the flow pattern of the liquid in the bed. For large-scale trickle bed, the dominant flow patterns are trickling flow and pulsing flow. The transition of pulsing for large particles is largely determined by inertial instabilities, and the flow map made by Charpentier and Favier [9], based on mass-flow rate, can be used to determine the transition of pulsing. Losey et al. [10] have performed a limited number of experiments indicating a different pulsing transition point for micro-packed beds in comparison to those in large-scale trickle beds. They explain that flow instabilities in the open channel upstream of their bed are the main cause of the pulsing. In the current work, the liquid is injected directly into the bed and as a result, no pulsing is observed. All our experiments are in the trickling range on the Charpentier map.

In the current micro-packed bed, with the Reynolds number in the order of magnitude of 1, inertia-induced pulsing is unlikely. Capillary forces are dominant and the most likely flow patterns are segregated and bubble flow. In the segregated-flow pattern, there is essentially a continuous path for the gas through the column, and the gas is allowed to bypass the liquid (gas-slip). In the bubble-flow pattern, the two phases move through the interstices of the bed as alternating packages. Capillary stresses cause the bubbles to expand towards the particles, pushing the liquid forward. As a result, gas-slip will be minimal and any stagnant liquid has difficulty to persist between the particles and the bubble train moving through the interstices.

For the bubble-flow pattern, the residence time of the gas and liquid will be the same, and the residence time can be estimated from the sum of the gas and liquid interstitial velocity. Fig. 5(b) shows that at low gas-flow rate, $\tau_L = L/(u_L + u_G)$. Fig. 5(a) shows that at high gas-flow rate the gas starts to bypass the liquid and the liquid-residence time is larger than it would be without bypassing.

Fig. 5(a) shows that a suitable correlation for the liquid-residence time (and hence the liquid-space velocity in kinetic experiments) can readily be constructed. For the HDS experiments, however, the bubble-flow pattern is preferred. The sulphur-containing components are volatile at HDS conditions, so these components might significantly evaporate to the gas phase and – in the case of the segregated-flow pattern – will leave the reactor with the fast-moving gas stream unconverted. Significant gas-slip, therefore, makes the kinetic experiments difficult to interpret, and has to be avoided. The RTD experiments in Fig. 5(b) indicate that at low gas-flow rate, gas and liquid move through the column together, and evaporation and condensation will not affect the residence time of the components of interest. As a result, it is prudent to perform the kinetic experiments at lower gas-to-liquid ratios than those typically applied in trickle beds as mentioned by Satterfield [6].

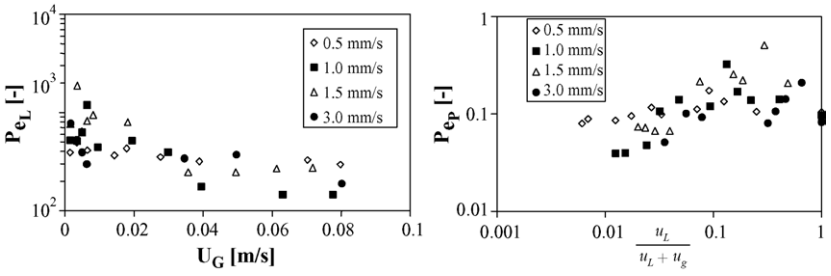

Fig. 6. Further processed data from gas/liquid experiments showing (a) the Péclet number (Pe_L as in Eq. (5)) vs. the gas-flow rate and (b) the particle Péclet number (Pe_p as in Eq. (6)) vs. the liquid fraction of the flow. The liquid-flow rates are indicated with different symbols.

5.3. Two-phase measurements—axial dispersion

The dimensionless width of the breakthrough curves is fairly constant for the measured residence-time distributions. The values of $Pe_p = 0.1$ are similar to the single-phase values. With the exception of single experimental points, all data are within $0.05 < Pe_p < 0.25$ (Fig. 6(b)). For kinetic experiments at high conversion, the column Péclet number is a more suitable parameter to consider. The values in Fig. 6(a) are all well above the rule-of-thumb criterion of $Pe_L > 100$ that is often used. There is some scatter in the data mostly due to small flow instabilities. Hysteresis effects have been avoided by performing all experiments in a pre-wetted column. The best way to reduce scatter for duplo or triplo experiments is to allow sufficient time for the flow to stabilise. For most measurements, about three residence times have been applied before starting an experiment. In kinetic experiments, a similar period is given to the reactor to stabilise after changing a set-point.

Applying the results directly to the context of this work, the measurement of HDS kinetics at high conversion levels, Eq. (8) prescribes the minimal reactor length. In an illustrative example, a 3000 ppm sulphur feed needs to be desulphurised to 30 ppm, i.e. 99% conversion. With the present scatter in the axial-dispersion data, it is prudent to take a safety factor 2 into account. With a particle Péclet number of 0.1, the minimal bed length is then 7 cm (Gierman, 10% max. deviation) or 18 cm (Mears, 5% deviation).

6. Conclusions

A method to quantify the plug-flow behaviour in small-scale packed beds has been derived. The RTD measurement shows sufficient plug-flow behaviour, as required for the work on deep HDS. It is found, however, that with increasing gas fraction in the flow, the bypass of the gas increases due to an segregated gas-flow pattern. At industrial conditions, sulphur-containing hydrocarbons may have fractions of up to 75% in the gas phase. Therefore, the gas rate should be kept low in order to limit the degree to which it bypasses the liquid. Neither the gas nor the liquid seems to influence the dimensionless liquid-residence-time distribution, making the residence time the most important parameter in the different experiments.

The RTD study provides valuable insight into the behaviour of scaled-down kinetic-test facilities.

Acknowledgements

The authors thank Shell Global Solutions and Albemarle Catalysts Company for financial support.

References

[1] J. Perez-Ramirez, R.J. Berger, G. Mul, F. Kapteijn, J.A. Moulijn, Catal. Today 60 (1–2) (2000) 93–109.
[2] M.T. Kreutzer, J.J.W. Bakker, F. Kapteijn, J.A. Moulijn, P.J.T. Verheijen, Ind. Eng. Chem. Res. 44 (2005) 4898.
[3] O. Levenspiel, Chemical Reaction Engineering, third ed., Wiley, NJ, 1999.
[4] D.E. Mears, Chem. Eng. Sci. 26 (1971) 1361.
[5] H. Gierman, Appl. Catal. 43 (2) (1988) 277.
[6] C.N. Satterfield, AIChE J. 21 (2) (1975) 209.
[7] E. Tsotsas, E.U. Schlünder, Chem. Eng. Proc. 24 (1) (1988) 15.
[8] J.R.F.G. de Carvalho, J.M.P.Q. Delgado, Chem. Eng. Sci. 60 (2) (2005) 365.
[9] J.C. Charpentier, M. Favier, AIChE J. 21 (6) (1975) 1213.
[10] M.W. Losey, M.A. Schmidt, K.F. Jensen, Ind. Eng. Chem. Res. 40 (12) (2001) 2555.